CONVECTION IN SPUTNIK PLANITIA, PLUTO: DEPTH OF THE N_2 ICE LAYER AND POSSIBLE PRESENCE OF BASAL N_2 MELT.
T. Wong[1], W. B. McKinnon[1], P. M. Schenk[2], J. M. Moore[3], J. R. Spencer[4], C. B. Olkin[4], L. A. Young[4], K. Ennico[3], H. A. Weaver[5], S. A. Stern[4], and the New Horizons Geology, Geophysics and Imaging Theme Team. [1]Washington University in St. Louis, Dept. of Earth and Planetary Sciences, St. Louis, MO 63130 (twong@levee.wustl.edu), [2]LPI, Houston, TX, 77058, [3]NASA Ames Research Center, Moffett Field, CA 94035, [4]SwRI, Boulder, CO, 80302, [5]JHUAPL, Laurel, MD 20723.

Introduction: The nitrogen-rich basin located in the left half of Pluto's heart-shaped region, informally named Sputnik Planitia (SP), spans ~900,000 km^2 and is 3.5 km below its surroundings. Images from the New Horizons feature show that the surface comprises of polygons that are about 10-40 km across, resembling the surface expression of convection [1-3]. It is thought that the layer or ice sheet sits within a broad impact basin formed in Pluto's water ice crust [3]. Based on the horizontal scale of the polygons, we perform convection calculations to constrain the depth of this N_2 layer and thus the depth of the Sputnik impact basin and related properties and conditions.

Nitrogen rheology: At laboratory conditions, solid N_2 exhibits ductile behavior down to 30 K [4], lower than the present annual time-averaged N_2-ice surface temperature of Pluto (~36 K). The upper limit (the melting temperature) is 63 K, and the corresponding temperature difference across the depth of the layer gives an upper bound of viscosity contrast of 2x10^5 for diffusion creep.

N_2 ice was predicted to deform in diffusion creep assuming similarity with the crystal structure and molecular bonding of solid methane [5]. Recent deformation experiments of solid N_2 ice suggest power-law creep with n=2.2 [4], plausibly in the grain-size sensitive regime [1,6]. At SP stresses and strain rates are lower than in the experiments, and the deformation mechanism is likely to transition from volume creep at higher temperatures to grain-boundary diffusion (n=1) at lower temperatures. Here we consider a Newtonian, but temperature dependent rheology in our simulations.

Frank-Kamenestkii approximation for viscosity: Viscosity is strongly temperature dependent and it assumes an Arrhenius form:

$$\eta = A \exp \frac{E}{RT} \qquad (1)$$

where A is a constant, E is the activation energy, and R is the gas constant. Due to this sensitivity to temperature, the viscosity contrast across the depth of the N_2 convecting layer can reach orders of magnitude even with a moderate temperature difference. High viscosity contrasts across the convecting cell are more difficult (but not impossible) to treat in numerical calculations. Thus the Arrhenius function for the viscosity is often linearized and approximated by an exponential function with the Frank-Kamenetskii parameter:

$$\theta = \frac{E\Delta T}{R{T_i}^2}, \Delta T = T_1 - T_0$$
$$\eta = A' \exp(-\frac{\theta T}{\Delta T}) \qquad (2)$$

where T_i, T_1, and T_0 are interior, bottom, and surface temperatures respectively.

The viscosity contrast calculated from Eq. 2 can be orders of magnitude smaller than from Eq. 1. While it is sufficiently accurate for the actively convecting interior of systems with large viscosity contrasts, the convective dynamics and scalings can be different [e.g., 7,8].

Convection regimes: In Fig. 1 we explore the parameter space given by a possible range of temperature difference across the SP convecting layer and taking E of N_2 ice in diffusion creep as 8.6 kJ/mol [5]. The Rayleigh number Ra is defined by the bottom viscosity; bottom (i.e. radogenic) heating is assumed in 12x1 2D boxes, with no horizontal slip at the base of the layer.

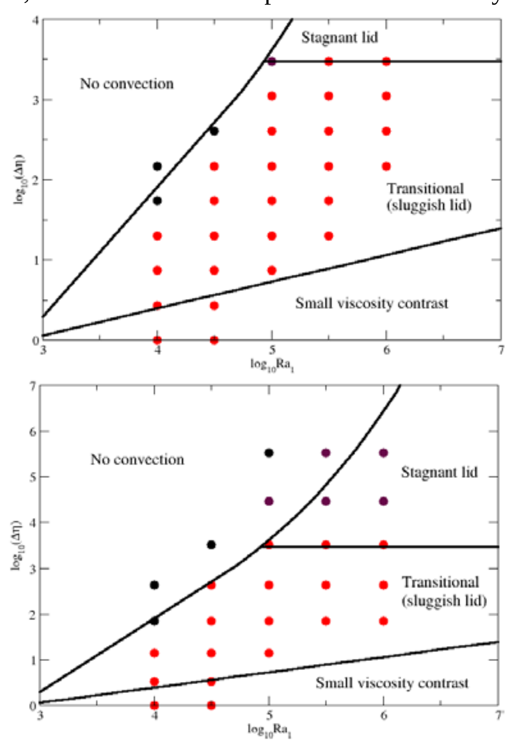

Fig. 1. The *Ra*-Δ*η* regime diagrams. Black dots: no convection; red: convecting systems that reached (statistically or periodically) steady-state; purple: weakly convecting systems. Top figure shows calculations in exponential viscosity, bottom figure in Arrhenius viscosity (note difference in vertical scales). Theoretical regime boundaries suggested by [9].

The moderate temperature difference between the surface temperature and the melting point of N_2 ice dictates that the range of possible viscosity contrasts between the top and the bottom of the SP convective layer. For exponential (FK) viscosity (Eq. 2), convection occurs in the mobile (small viscosity contrast) or the sluggish lid regime (transitional). However the Arrhenius viscosity law (Eq. 1) gives a wider range of viscosity contrast so that all regimes of convection are possible. We note that although the regime boundaries in Fig. 1 are derived for exponential viscosity, it generally agrees with the transitions for viscosity contrasts in for the Arrhenius function.

Regime transitions. Convective dynamics are complicated at the vicinity of regime transitions [10]. At low *Ra* and low $\Delta\eta$ near the transition between no convection and sluggish/mobile lid regime, the initial perturbation wavelength affects the onset of convection and also the number of plumes or aspect ratios of the cells if the system is convecting. What this means in the real world of Pluto is that initial conditions, or convective history, is important. The transition between sluggish lid and stagnant lid is less well-defined and has a wide range of behavior. The plumes may move horizontally in one direction continuously or in steps, or oscillate around a mean position, and in some cases plumes are continuously created and merge. The horizontal movements of plumes can have different speeds depending on the aspect ratio of the convective box.

Bottom boundary condition: solid H_2O bedrock or nitrogen ice melt? The conditions at the base of the N_2 layer are uncertain. The temperature of the surface of the water ice may exceed the melting point of N_2 ice. The bottom boundary conditions affects the onset of convection and also the resulting heat flow [11]. We investigate both free-slip and no-slip bottom boundary conditions corresponding to a bottom with melt or with water ice. Free-slip bottom boundaries increase the heat flow and higher surface velocities by up to 50%, and push the critical Rayleigh number lower. For a case with high Rayleigh numbers and moderate viscosity contrast (*Ra*=10^6, θ=8 or $\Delta\eta \approx 3e3$), the aspect ratios of convective cells is further increased from 3 to 6 in 2D simulations. In 3D simulations (Fig. 2) the increase in plume size is dramatic, in agreement with the simulations of [12]. Liquid N_2 is less dense than the solid, so could even erupt to the surface of SP.

Depth and basal conditions of SP: The basal temperature of the N_2 layer controls the viscosity contrast $\Delta\eta$ and *Ra*. If the basal temperature of the N_2 ice is lower, both *Ra* and the viscosity contrast will be smaller, shifting the relevant parameters for SP on Fig. 1 towards the bottom left. At 63 K, $\Delta\eta$ reaches $\approx 2x10^5$ in Arrhenius form, and weak convection requires depths > 3 km.

Elongated convective cells also require a higher *Ra* for larger viscosity contrasts to be in the sluggish/mobile lid regime. N_2 melting at the bottom may allow larger convective aspect ratios, meaning that the implied depth of the SP N_2 layer from the observed cells may less than thought. However, as the temperature difference (and thus $\Delta\eta$) are maximized for basal N_2 melting, it may require a larger *Ra* for large aspect ratio cells. From this we infer a minimum depth of > 4 km to have sluggish lid convection, as smaller depths (although possible with the larger aspect ratio) will not give a sufficiently large Ra for wide cells. We continue to explore the planforms of 3D convection.

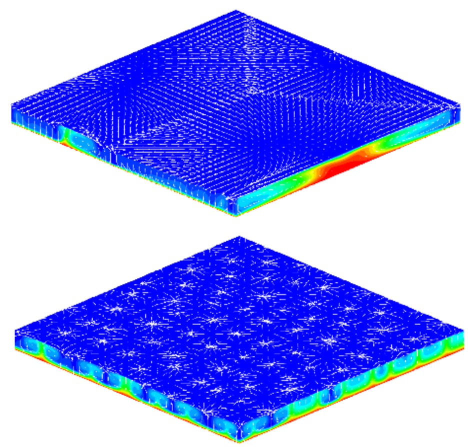

Fig. 2. 3D simulations in 12x12x1 box with Ra=3x10^5, θ=6 ($\Delta\eta \approx 400$) and exponential viscosity. Top figure has free-slip bottom boundary, bottom figure has no-slip boundary. The surfaces of both cases are free-slip. Color scale shows temperature (blue=cold, red=hot), white arrows are velocity vectors with length indicating magnitudes.

References: [1] McKinnon, W.B. et al. (2016) *Nature*, 534, 82-85. [2] Stern, S.A. et al. (2015) *Science*, 350, 10.1126/science.aad1815 [3] Moore, J.M. et al. (2016) *Science*, 351, 1284-1293 [4] Yamashita, Y. et al. (2010) *Icarus*, 207, 972-977. [5] Eluszkiewicz, J. & Stevenson, D.J. (1990) *GRL*, 17, 1753-1756. [6] Goldsby, D. L. & Kohlstedt, D. L. (2001) *JGR*, 106, 11017-11030. [7] Korenaga J. (2009) *GJI*, 179, 154-170. [8] Stein, C. & Hansen, U. (2013) G3, 14, 2757-2770. [9] Solomatov, V.S. (1995) *Phys. Fluids*, 7, 266-274. [10] Kameyama, M. & Ogawa, M. (2000) *EPSL*, 180, 355-367. [11] Stengel, K.C. et al. (1982) *J. Fluid Mech.*, 120, 411-431. [12] Tackley, P.J. (1993) *GRL*, 20, 2198-2190.